Contactless Position Sensing and Control of Pneumatic Cylinders using a Hall Effect Sensor Array

Tim Hojnik[1,2], **Paul Flick**[1], **Jonathan Roberts**[2]
[1] Cyber-physical Systems, Commonwealth Scientific and Industrial Research Organisation
[2] Science and Engineering Faculty, Queensland University of Technology

Abstract

This paper proposes an accurate position sensing method and subsequent positional control for pneumatic actuators. An array of hall effect sensors is used to allow contactless sensing of the flux field produced by a magnet located inside most pneumatic cylinders. The hardware functions conjointly with the proposed algorithm that fuses the sensor data and determines the piston position through predefined mathematical functions produced by data analyses and careful sensor calibration. The hall effect sensors used have a high sensitive dependence on initial conditions, due to the fundamental non-linearity of the equations describing their response, therefore careful system identification and numerical model validation was performed. Preliminary solenoid valve controllers are proposed, allowing for full positional control of pneumatic pistons and location stabilization. This extends the uses of such actuators further than currently accustomed, and allows a cylinder to act as a linear actuator that exhibits compliant behaviour due to the underlying compressibility of air.

1 Introduction

Pneumatic actuators of a variety of forms and sizes are commonly used for factory automation, passive suspension for automotive and railway vehicles, construction robotics, robotic arms and recently as artificial muscles for humanoid robots [Docquier *et al.*, 2007; Choi *et al.*, 2005; Tondu *et al.*, 2005; Zhu *et al.*, 2008]. Pneumatic cylinders are inexpensive, safe, and have a high power to weight ratio, making them very attractive to researches and industry [Bone and Ning, 2007]. The standard industry control for these actuators is through the use of a solenoid valve, turning the airflow to the cylinder on or off, as desired.

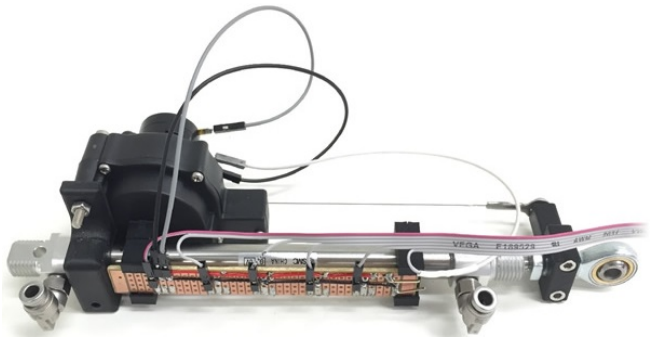

Figure 1: String transducer and Hall Effect sensors array mounted onto a pneumatic cylinder, for gathering data and piston control.

Due to this on/off switching, the current control standard is limiting as only two positional states are easily achievable, fully retracted or fully extended [Ali *et al.*, 2009]. It is difficult to control the exact position of the piston inside these cylinders, especially ones with small stroke ($< 200mm$) because of the limited control allowed by solenoid valves. An accurate feedback loop must therefore be present to allow for accurate positional control of the piston. However, this position sensing for small cylinders is not readily available in a small package as currently only discrete, digital, sensors can be purchased from suppliers, therefore a high frequency and accurate device is needed for the piston position feedback to a controller for accurate positional control. Components such as a string transducer or linear potentiometer can solve this problem, however are generally large, heavy and very costly, making them unattractive to many users. Furthermore, wear and tear becomes an issue with continued use as frictional forces are experienced by these devices.

Factors such as the fundamental non-linear response characteristics of pneumatics and in turn their compliant behaviour add complexity to this control and sensing problem [Kumar *et al.*, 2013], although this compliant behaviour exhibited by pneumatics is what makes

them attractive to many users to begin with. In contrast, hydraulic and electric linear actuators demonstrate rigid behavior and can only act in a compliant manner through the use of convoluted feedback control strategies [Daerden and Lefeber, 2002]. The compliant behavior in pneumatic systems is present due to the compressibility of air, and is directly proportional to the operating pressure supplied to the cylinder, which can therefore easily be controlled through a pressure regulator situated in line of the airflow. The ease of compliant factor control together with aforementioned properties makes pneumatics attractive for a variety of uses however, the limiting control provides a substantial limitation for further, more delicate uses.

This paper proposes an accurate method for determining the piston position at any instance in its stroke, acting as an analog position rather than a digital position sensor, unlike ones currently available on the commercial market. The knowledge gap previously present in accurate, easy and fast pneumatic piston position sensing is filled. Solutions for preliminary controllers are also proposed, alongside results gathered from preliminary experiments to compare different types of controllers. The research proposed in this paper provides a system that is simply added onto existing pneumatic cylinders, with no modification to the cylinder required where a magnet is present in the cylinder. This makes it cost effective, and combines the most desirable properties of electric linear actuators, hydraulics and pneumatics to expand the usability of pneumatics to more delicate uses such as robotic arms or artificial muscles in humanoid robotics.

2 Background

In this section, we discuss the background theory of the components used in this research and give an overview of the hardware configuration of the proposed system.

2.1 Pneumatic Cylinder

Pneumatic cylinders work by enclosing a piston inside a cylinder and have two separate air compartments, as air flows into one, the other is bled and as a result the inside piston changes position. The speed of this movement can be controlled by the air pressure applied from an external driving source. Due to this external energy source, the cylinders are often light weight and have an exceptionally high energy density as the energy storage is kept and controlled externally to the cylinder. Pneumatic cylinders have a single degree of freedom, as they are capable of moving their piston along a linear axis, when air is supplied.

2.2 String Transducer

A string transducer is a linear device that varies the resistance over its poles proportionally to the length that its cable is drawn. This acts as a variable resistor and the draw of its cable can be measured using an ADC device. It is primarily used for positional measurement and as so was used as a ground truth for this research as it was easily mounted to the external casing of the cylinder.

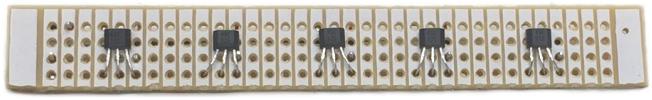

Figure 2: Hall effect sensors mounted in an array over 80mm, allowing for positional readings over 100mm. Sensors are spaced evenly to ensure sensor reading overlap.

2.3 Hall Effect Sensor

A hall effect sensor is a transducer that varies its output voltage in response to a magnetic field. The sensor is designed to read the magnetic flux in its immediate environment, as a result the sensors are commonly used for a variety of contactless sensing applications such as proximity sensing, positioning, revolution measurement (as tachometer), and electrical current sensing applications. These devices are readily available, cost effective and are solid state, therefore have a long and reliable working life as no wear and tear other than that of current passing thought the terminals is experienced. The sensors draw low current at nominal operation and most can generally be sampled at very high frequencies of up to 25 kHz [Pepka, 2007].

Hall effect sensors were chosen for this application primarily due to their contactless sensing ability, allowing us to utilize the existing magnet inside of pneumatic pistons. This limits the need for any internal cylinder modification, and allows the system to be added onto almost any cylinder without modifications to the cylinder structure.

Sensor Types

A variety of hall effect sensors exist that can be used to sense the position of a magnet. Unipolar and Bipolar sensors detect a single and double magnetic pole, respectively. However provide a digital output where analogue is desired. These types of sensors were undesired as an analog response is required for determining the continuous position of a magnet.

Linear sensors however, function using the ratiometric principle, outputting a ratio of the input voltage with respect to the field strength applied. These sensors detect both the south and north magnetic fields and output an analog reading. This technology provides an effective solution for the desired contactless sensing application,

after requirements such as sensor resolution, accuracy, cost and effective operating distance have been met.

Effective Air Gap

The air gap of the hall effect sensors refers to the gap between the surface of the sensor, and the surface of the magnet. An inversely proportional relationship is exhibited between the air gap and the magnetic flux density measured by the sensors. The Effective Air Gap (EAG) of the sensor is therefore the distance between the magnet and the sensor that allows for optimal readings to be recorded. The EAG varies depending on the sensor type, model and on the physical properties of the magnet, such as its size and strength. As the relationship between the field strength reading and the distance of an air gap is exponential, choosing the correct air gap is important. The maximum reading returned by the sensor at any air gap can be determined using

$$F_X = \frac{B_r}{2}\left[\left(\frac{L+X}{(R^2+(L+X)^2)^{-2}}\right) - \frac{X}{(R^2+X^2)^{-2}}\right] \quad (1)$$

where F_X is the field strength in (Gauss), B_r is the Residual Magnetic Inductance (Gauss), L is the length of the magnet (mm), X is the air gap (mm) and R is the radius of the magnet (mm).

After the maximum field strength reading by the sensor has been determined for a range of air gaps, the appropriate maximum reading can then be chosen and the EAG determined via choosing the air gap inputted into the equation that corresponds to the chosen field strength.

3 Sensing & Data Analyses

This section describes the physical configuration of the proposed positional sensing system, data collection and analyses methods alongside visual representation of the data presented for clarity.

3.1 System Overview

A photo of the proposed sensing system can be seen in Figure 1, mounted in a desired configuration to the external casing of a cylinder. This consists of an array of hall effect sensors mounted onto a circuit board, which is then mounted to a pneumatic cylinder via 3D printed mounts. The signal from each hall effect sensor then runs to an off-board microcontroller with a built in ADC. A string transducer is also mounted onto the external body of the cylinder and is shown in the left of the image, used for hall effect sensor calibration, and as ground truth during the data collection process.

3.2 Pneumatic Cylinder

A pneumatic cylinder with $100mm$ stroke was chosen for this research as this length is commonly used in industry automation and has recently been researched. The cylinder has a diameter of $11mm$ and an overall length of $190mm$. Due to the cylinders pressure ratings, pressure between $200 - 800kPa$ was used, varying when appropriate.

3.3 String Transducer

A string transducer was used for the calibration of the hall effect sensors and as a ground truth for gathering data. Mounted securely to a 3D printed bracket that fits around the cylinder casing to hold it in place. An accuracy of 0.28 mm was achieved with the use of a 10-bit ADC for initial testing, however this is aimed to improve by implementing a 16-bit ADC in future work.

3.4 Microcontroller

A microcontroller with a built in ADC was used. This provided 10-bit resolution and sampling frequency of up to $1000Hz$, although $100Hz$ was found to be sufficient for running the algorithm. All data was recorded and processed at $1000Hz$ for best results.

3.5 Circuit Board and Mounting

The efficiency and accuracy of the algorithm discussed in this paper is dependant on the precision of the known sensor mounting locations. For this reason, a custom board was designed as well as a 3D printed mount that secures the board to the pneumatic cylinder. This allowed for accurate placement of the hall effect sensors, and known[1] distance between each sensor. This is shown in Figure 2, with five hall effect sensors mounted equal distances apart. The position of hall effect sensors is very important to the accuracy of the results, refer to the calibration section of this paper for an explanation of the calibration procedure.

3.6 Hall Effect Sensor Calibration

The chosen sensors are not vulnerable to most environmental disturbances that may affect other commonly used sensors such as vibration, moisture, ambient light, temperature, etc [Gilbert and Dewey,]. As these sensors are contactless, they are also immune from interference of dirt or dust build up on their casings.

Initial Sensor Position Calibration

Position calibration was only performed once, to determine the sensor mounting positions with respect to the piston stroke. This spacing between each hall effect sensors is not required to be equal, nor manually measured,

[1]Mounting positional error can be facilitated for in the algorithm during the calibration process.

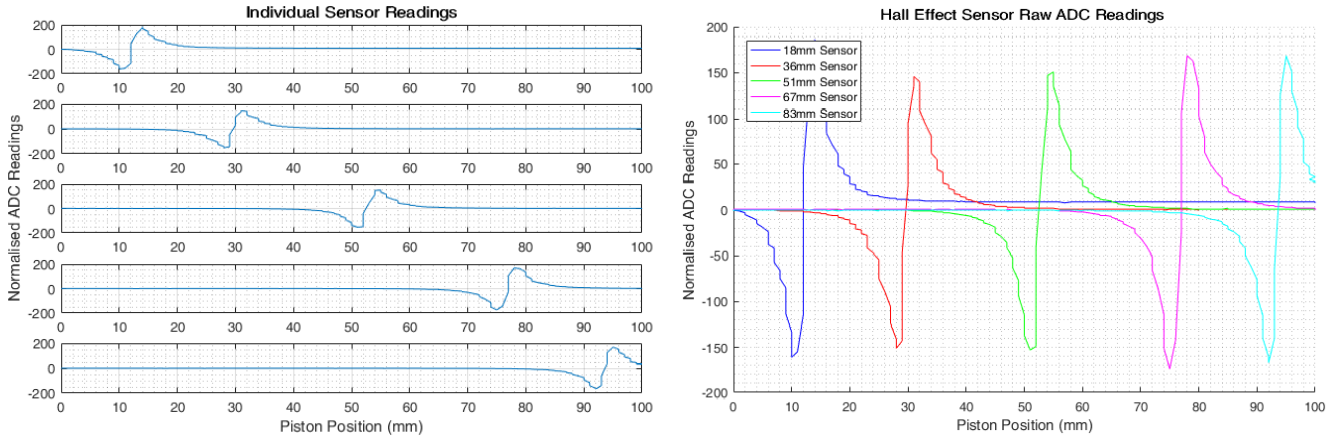

(a) (b)

Figure 3: (a) Hall effect sensors normalised response to magnet moving through their sensing range recorded simultaneously. (b) Hall sensor readings as the piston moves from fully contracted to fully extended $(0 - 100mm)$ plotted on the same axis to clearly show sensor reading overlap.

provided that a calibration element such as a string potentiometer is present. The positions of each sensor can be determined to great precision by calibrating the hall effect sensors against the string potential positional reading. The length of the magnet can then also be determined from this data, as the linear response of each sensor immediately between its minimum and maximum readings is directly proportional to the length of the magnet. This linear area of the sensor response can be seen in Figures 3a and 3b.

Normalization Calibration

A normal sensor reading calibration is performed at each power-on cycle, this is the only calibration needed[2] to calibrate the flux density readings. As the ambient magnetic field reading is different in all locations, an automatic calibration script was written and automatically ran when the system was powered on.

The sensor power on time is less than $4\mu s$, and as they are capable of sampling at a rate of up to $25kHz$, the calibration process is completed in minimal time. Once the system was powered on, 20 readings over a time frame of one second were recorded, then averaged. This was done simultaneously for each individual sensor. The sensors did not demonstrate any drift in the readings over time, therefore a single calibration proved sufficient for this application.

4 Sensor Response Modelling

Once the hall effect sensors were mounted at their desired positions, they were calibrated to account for any environmental interference. As the ADC used has an accuracy of 10 bits, a value between 0 and 1023 was returned by each sensor. The linear hall effect sensors used are capable of measuring the north and south poles of the magnet, as a result the floating reading they return with no substantial field present was 511. This was expected as the reading is in the middle of the ADC range. A reading of 0 or 1023 correspond to the maximum south and maximum north readings, respectively.

The readings from all sensors were simultaneously recorded, and the piston moved from one extremity to another. This data was then plotted for a visual representation of the sensor response. The raw, normalised data is shown is Figure 3a, and in Figure 3b plotted on the same axis to clearly show the sensor overlap.

Figure 3b demonstrates that at any given time, at least two sensors are detecting the magnet inside the cylinder. This is important as the response given from a single sensor has two positional locations for one ADC reading. This is visible on the graph between the sensors minimum and maximum reading, when the magnet is exactly over the sensor. As a result of this characteristic in the curve, a minimum of two hall effect sensors are required to accurately determine the position corresponding to a single ADC reading.

4.1 Look-up Table

For initial testing, a look-up table was constructed from the recorded data. This allowed for a time efficient way to test the principle and prove the concept of using analog hall effect sensors for piston position detection. This approach was limiting as only predetermined, discrete positions were able to be returned and the table required

[2]Temperature calibration is performed within the sensor automatically.

substantial storage space on the microprocessor. Therefore, a mathematical function was fitted to the data instead, explained in the following sections.

4.2 Non-linear Response Modelling

A number of aforementioned tests were performed to obtain an acceptable amount of data of the sensor response to a varying magnetic flux field. This data was then averaged and used for function fitting. A number of functions were tested and resulted in the finding that a negative exponential and a positive exponential functions fit the south and north magnetic field responses best, respectively.

The exponential function segment of the sensor response was mapped and used to determine the piston position. This response is present immediately before the minimum reading of the sensor, and immediately after the maximum reading, until the flux field is fully removed. Therefore these responses can be accurately mapped to an exponential function in the form of

$$y = ae^{bx} + z, \qquad \forall x, y \tag{2}$$

where y is the sensor reading (ADC), x is the displacement (mm), a and b are scaling factors, and z is the y intercept. As we want to find the horizontal displacement of the piston from the hall sensors, rearranging the function with respect to x gives

$$x = \frac{log_{10}(\frac{y-z}{a}) + 2i\pi n}{b}, \qquad n \epsilon Z \tag{3}$$

where $a \neq 0$, $b \neq 0$, $z \neq y$. Due to the use of DC signals, further simplification of equation 3 is required to eliminate the imaginary numbers. As a result rearranging for real numbers domain only within a desired range gives

$$x = \frac{log_{10}(\frac{y}{a})}{b}, \tag{4}$$

where $a \neq 0$, $b \neq 0$, $y \neq 0$. Equation 4 is then used to map the non-linear sensor response to a linear distance. The distance found is relative to the sensor and is therefore with respect to a different frame of reference than the piston. To transform it to the reference frame of the piston, the calculated distance needs to be added to the fixed, known position of the hall effect sensor as follows

$$x_{piston} = S_i + x, \qquad -S_R \leq x \leq S_R \tag{5}$$

where x_{piston} is the position of the piston along its stroke (mm), S_i is the fixed hall effect sensor position along the piston stroke (mm), x is the piston position with respect to the sensor S_i and S_R is the range of the sensor (mm).

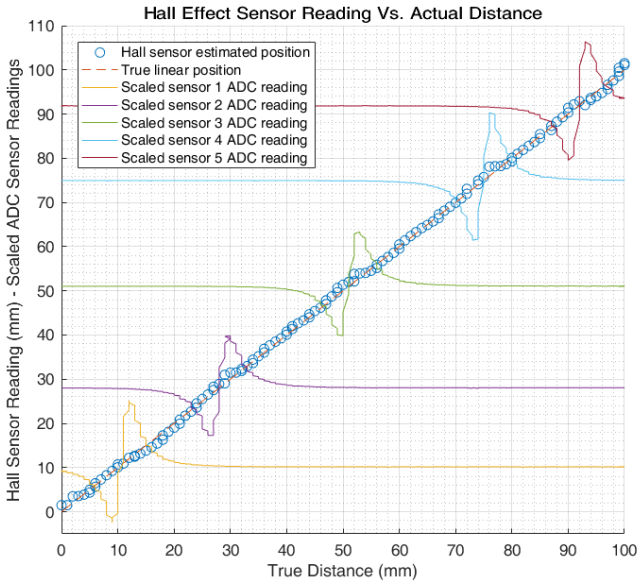

Figure 4: This figure shows the algorithm's distance calculation with respect to the true distance of the cylinder. Each hall effect sensor's response is overlaid for extrapolation.

Equation 5 describes how the position of the piston can be determined with respect to only one sensor. However, this approach only works while the magnet is within the sensor range. For an array of sensors, the two sensors with the highest ADC readings were used while others were disregarded for that single reading as they likely did not detect the magnet. These two sensor ADC readings are used to calculate the piston position, then the average of the two readings is calculated and returned as the final result.

4.3 Linear Response Modelling

Furthermore to the non-linear response modelling, the linear response can also be modelled provided the physical characteristics allow. The length of linearity between the sensor minimum and maximum readings is directly proportional to the length of the magnet. Therefore, for magnets of substantial lengths, this linear section of the function can also be mapped directly to a linear function in the form of

$$y = mx + c, \qquad \frac{-L}{2} \leq y \leq \frac{L}{2} \tag{6}$$

where L is the length of the magnet (mm), y is the sensor reading (ADC), x is the horizontal displacement (mm), m is the gradient and c is the y intercept.

Rearranging the function to give the horizontal position of the cylinder then takes the form of

$$x = \frac{y - c}{m}, \qquad m \neq 0, (y - c) \neq 0 \tag{7}$$

This linear property of the sensor response is desirable if design considerations can be made to allow the use a long magnet. In this case, the sensor spacing is also directly proportional to the length of the magnet, as only one sensor is required to give accurate position of the piston.

The magnet present in the cylinder used was only $2mm$ wide, therefore this linear response was not used for positional calculations as a range of only $2mm$ per sensor could be achieved.

4.4 Filtering

A low-pass filter was added to the system to control the outliers in the returned positional readings. An RC low-pass filter was modelled in the algorithm using a first order, single pole filter in the form of

$$y(n) = Ax(n) - By(n-1), \tag{8}$$

where $y(n)$ is output, $x(n)$ is input, $y(n-1)$ is the output at the previous time step and A and B are scaling factors [Sedra and Brackett, 1978].

This filtering was then applied to the ADC signal, before the data was processed, to determine the position. Using the filter resulted is a smoother response and more accurate positional estimates, Figure 4 shows the results after the filtering was applied.

4.5 Function Fitting

The exponential and linear functions discussed in the previous sections were fitted to the sensors response using Matlab. Initial raw data from all the sensors was recorded a number of times at $1000Hz$, then averaged to obtain the general response of the sensors. Once the function was generated, it was then programmed into the algorithm to calculate the piston positional estimates. No further modification to the function was required as this process was only completed initially to map the sensor responses to a mathematical function. This ensured the response of all the sensors was mapped correctly for positional estimation.

5 System Control

This section describes the control techniques used to control the piston position. The control of pneumatic cylinders is difficult, due to the non-linear properties demonstrated by the systems [Carneiro and de Almeida, 2006]. The compressibility of air, system compliance, air leakage, varying air pressure, airflow through the valve and end of stroke inactive volume due to cushioning contribute to the non-linear properties of the system. Therefore a controller needs to accurately model these factors, to work efficiently. However if a strong feedback loop is present these non-linear factors can be accounted for in the next time step, and the control system can be simple such as bang-bang or fuzzy logic [Krener, 1974; Hosovsky *et al.*, 2014; Berenji, 1992]. Refer to [Taleb *et al.*, 2013] and [Van Varseveld and Bone, 1997] for other good control methods in robotics.

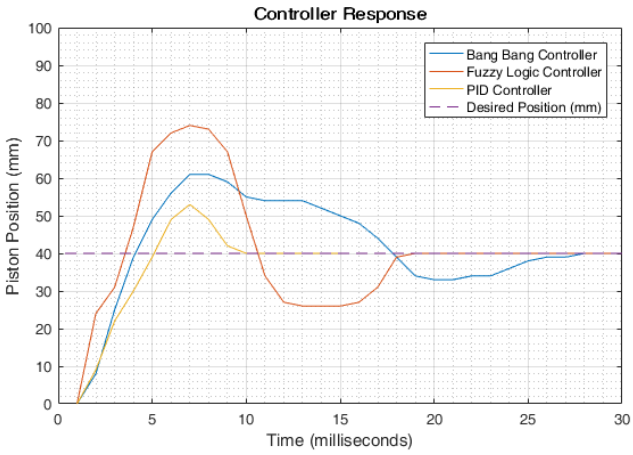

Figure 5: Bang Bang, Fuzzy Logic and PID controller responses in moving the piston from 0mm to 40mm in as least time as possible. Operating pressure of 450kPa with no load on the cylinder.

5.1 Bang-bang

Initial proof of concept was demonstrated with a simple bang-bang controller. The hysteresis controller switched abruptly between two states to control the on-off solenoids, which in turn controlled the airflow to the pneumatic cylinder. The response observed from the controller was plotted and can be seen in Figure 5. The controller demonstrates a 45% overshoot and a settling time of 27 milliseconds. It can also be seen that the controller is under-damped as some oscillation is present before the system settles.

Limitations of control were found when performing initial tuning. The air pressure and the switching time of the solenoid demonstrated a direct relationship, until the physical limits of airflow were approached. The solenoid valve has a finite size channel for the airflow, therefore only a set volume of air can flow through. It was demonstrated that when the air pressure was increased, more air volume was able to flow, therefore the amount of time the valve was opened for could be decreased. This relationship is presented in Table 1.

The physical limitations of the system are reached when the switching time is less than 3 milliseconds. At this rate the volume of airflow through the valve is insufficient to move the piston. Similarly, when the air pressure is too low, the switching time becomes irrelevant as the pressure is unable to move the piston.

Table 1: Switching Time with Respect to Operating Air Pressure

Operating Pressure (kPa)	Min Switching Time (ms)
200	6
300	4
450+	3

5.2 Fuzzy Logic

A fuzzy logic controller was then implemented to test the effectiveness of varying the time that the solenoid is turned on, proportional to the distance the piston needed to travel to reach its desired position. This was done by measuring the current position of the piston and comparing it to the desired position, then scaling the amount of time the solenoid remains turned on by the size of the distance it needed to travel. Similar to bang bang control, this algorithm deals with on and off states for the solenoid, however the fuzzy logic allows to set states to partially on and partially off. Furthermore, as the solenoid only has two finite states, the partially on and partially off states were translated into the amount of time the solenoid needs to remain on or off. This resulted in faster settling time than bang-bang control, but in greater overshoot as the system overestimated the time the solenoid needs to remain on for.

5.3 Proportional, Integral & Derivative

A proportional, integral and derivative (PID) controller was also implemented to control the position of the piston. A PID controller is a common, yet effective control method for controlling a variety of variables, that can be tuned to yield desired overshoot, rise and settling time [Åström and Hägglund, 2006]. A conventional PID controller can be designed using

$$u(t) = K_p e(t) + K_i \int_0^t e(t)dt + K_d \frac{d}{dt} e(t), \qquad (9)$$

where $u(t)$ is the output, $e(t)$ is the input and K_p, K_i, K_d are the proportional, integral and derivative controller gains, respectively. As a PID is designed to output an analog value, and the solenoids only take digital, a conversion needed to be made to allow control of the solenoids. This was done using time proportioning control (TPC) with the implementation of a low frequency Pulse Width Modulation (PWM) controller. The PID outputs a value between 0 and k where the solenoid only takes 0 or 1, we were able to vary the time that the solenoid valve was turned on for, controlling the volume of air that the cylinder receives. As a result, logic was added to control the solenoid 'on' time, proportional to the controller output.

The response of this control method can be seen in Figure 5. The figure demonstrates undesirable overshoot, however the controller performs substantially better than bang-bang or fuzzy logic, as expected. The overshoot and other factors can be adjusted by further tuning of the K_p, K_i, K_d gains in equation 9 to produce desired results.

6 Conclusion

This paper overviews an accurate sensing system for pneumatic cylinders using an array of sensors that can be mounted to the external casing of a cylinder, with no modification required provided a magnet is present inside the cylinder. The hall effect sensors used enable high frequency and accuracy sampling of the flux field produced by the magnet moving on a linear axis. The contactless sensing ability of the sensors allow the system to experience no physical wear or tear, as no sensor touches a moving surface. As a result increasing the usability of pneumatic cylinders to applications that require accurate control such as robotic arms, actuators for humanoid robots, factory automation and any other applications that require a fast linear rate of positional change and high energy density in a small and lightweight package.

References

[Ali *et al.*, 2009] Hazem I Ali, SBBM Noor, SM Bashi, and MH Marhaban. A review of pneumatic actuators (modeling and control). *Australian Journal of Basic and Applied Sciences*, 3(2):440–454, 2009.

[Åström and Hägglund, 2006] Karl Johan Åström and Tore Hägglund. *Advanced PID control*. ISA-The Instrumentation, Systems and Automation Society, 2006.

[Berenji, 1992] Hamid R Berenji. Fuzzy logic controllers. *An introduction to fuzzy logic applications in intelligent systems*, pages 69–96, 1992.

[Bone and Ning, 2007] Gary M Bone and Shu Ning. Experimental comparison of position tracking control algorithms for pneumatic cylinder actuators. *IEEE/ASME Transactions on mechatronics*, 12(5):557–561, 2007.

[Carneiro and de Almeida, 2006] J Falcão Carneiro and F Gomes de Almeida. Reduced-order thermodynamic models for servo-pneumatic actuator chambers. *Proceedings of the Institution of Mechanical Engineers, Part I: Journal of Systems and Control Engineering*, 220(4):301–314, 2006.

[Choi *et al.*, 2005] Hyeun-Seok Choi, Chang-Soo Han, Kye-young Lee, and Sang-heon Lee. Development of

hybrid robot for construction works with pneumatic actuator. *Automation in Construction*, 14(4):452–459, 2005.

[Daerden and Lefeber, 2002] Frank Daerden and Dirk Lefeber. Pneumatic artificial muscles: actuators for robotics and automation. *European journal of mechanical and environmental engineering*, 47(1):11–21, 2002.

[Docquier *et al.*, 2007] Nicolas Docquier, P Fisette, and H Jeanmart. Multiphysic modelling of railway vehicles equipped with pneumatic suspensions. *Vehicle System Dynamics*, 45(6):505–524, 2007.

[Gilbert and Dewey,] Joe Gilbert and Ray Dewey. Linear hall-effect sensor ics. Allegro MicroSystems LLC.

[Hosovsky *et al.*, 2014] A Hosovsky, P Michal, M Tóthová, and O Biros. Fuzzy adaptive control for pneumatic muscle actuator with simulated annealing tuning. In *Applied Machine Intelligence and Informatics (SAMI), 2014 IEEE 12th International Symposium on*, pages 205–209. IEEE, 2014.

[Krener, 1974] Arthur J Krener. A generalization of chow's theorem and the bang-bang theorem to nonlinear control problems. *SIAM Journal on Control*, 12(1):43–52, 1974.

[Kumar *et al.*, 2013] Vikash Kumar, Zhe Xu, and Emanuel Todorov. Fast, strong and compliant pneumatic actuation for dexterous tendon-driven hands. In *Robotics and Automation (ICRA), 2013 IEEE International Conference on*, pages 1512–1519. IEEE, 2013.

[Pepka, 2007] Gary Pepka. Position and level sensing using hall-effect sensing technology. *Sensor Review*, 27(1):29–34, 2007.

[Sedra and Brackett, 1978] Adel S Sedra and Peter O Brackett. *Filter theory and design: active and passive*. Matrix Pub, 1978.

[Taleb *et al.*, 2013] Mohammed Taleb, Arie Levant, and Franck Plestan. Pneumatic actuator control: Solution based on adaptive twisting and experimentation. *Control Engineering Practice*, 21(5):727–736, 2013.

[Tondu *et al.*, 2005] Bertrand Tondu, Serge Ippolito, Jérémie Guiochet, and Alain Daidie. A seven-degrees-of-freedom robot-arm driven by pneumatic artificial muscles for humanoid robots. *The International Journal of Robotics Research*, 24(4):257–274, 2005.

[Van Varseveld and Bone, 1997] Robert B Van Varseveld and Gary M Bone. Accurate position control of a pneumatic actuator using on/off solenoid valves. *IEEE/ASME Transactions on mechatronics*, 2(3):195–204, 1997.

[Zhu *et al.*, 2008] Xiaocong Zhu, Guoliang Tao, Bin Yao, and Jian Cao. Adaptive robust posture control of a parallel manipulator driven by pneumatic muscles. *Automatica*, 44(9):2248–2257, 2008.